Genetically Encoded Fluorescent Biosensor for Rapid Detection of Protein Expression

Matthew G. Eason, Antonia T. Pandelieva, Marc M. Mayer, Safwat T. Khan, Hernan G. Garcia, and Roberto A. Chica*

Read Online

ACCESS | Metrics & More | Article Recommendations | Supporting Information

ABSTRACT: Fluorescent proteins are widely used as fusion tags to detect protein expression *in vivo*. To become fluorescent, these proteins must undergo chromophore maturation, a slow process with a half-time of 5 to >30 min that causes delays in real-time detection of protein expression. Here, we engineer a genetically encoded fluorescent biosensor to enable detection of protein expression within seconds in live bacteria. This sensor for transiently expressed proteins (STEP) is based on a fully matured but dim green fluorescent protein in which pre-existing fluorescence increases 11-fold *in vivo* following the specific and rapid binding of a protein tag (K_d 120 nM, k_{on} 1.7×10^5 M^{-1} s^{-1}). In live *E. coli* cells, our STEP biosensor enables detection of protein expression twice as fast as the use of standard fluorescent protein fusions. Our biosensor opens the door to the real-time study of short timescale processes in live cells with high spatiotemporal resolution.

KEYWORDS: *protein engineering, green fluorescent protein, protein−peptide interaction, fluorescence*
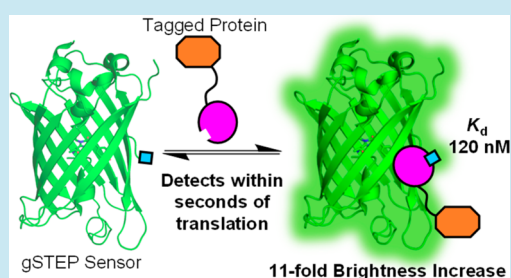
*A*equorea victoria green fluorescent protein (GFP) and its variants are widely used as quantitative reporters of gene expression to uncover the underpinnings of endogenous and synthetic genetic circuits.[1−3] To become fluorescent, these proteins undergo chromophore maturation, an autogenic process that begins immediately following folding and involves successive steps of protein backbone cyclization, dehydration, and oxidation.[4] The rate of chromophore maturation is highly dependent on temperature, pH, and oxygen concentration, which leads to large variations in half-times depending on experimental conditions.[5] Under optimal conditions, maturation half-times for GFPs range from 5 to >30 min in *E. coli*.[5] These maturation half-times are too slow for quantitative detection of fast biological processes occurring within a few minutes, such as those involving transiently expressed or fast-degrading proteins with half-lives of less than 5 min.[6,7] As a result, accurate quantification of these proteins at a given point in time often requires *post hoc* mathematical transformations to correct delays in detection of protein expression caused by chromophore maturation.[8−10]

To minimize the delay between translation and detection of a protein of interest, biosensors that translocate a pre-expressed and fully matured fluorescent protein from the cytosol to the nucleus following expression of a protein of interest have been developed.[11,12] However, the need for translocation prevents these biosensors from directly detecting proteins in the cytoplasm, and renders then unusable in bacteria. Other biosensors use a repeating peptide fusion tag on the protein of interest to recruit multiple copies of a pre-

expressed and fully matured cytosolic GFP, leading to the formation of large fluorescent aggregates that can be detected by fluorescence microscopy.[13−15] While these biosensors enable real-time imaging of protein expression in individual cells, their large size (>1 MDa) can interfere with the physical properties of the protein of interest. Therefore, an ideal biosensor for the rapid detection of protein expression *in vivo* would not only minimize the delay between translation and detection of the protein of interest, but would also not require translocation of the fluorescent protein into a different subcellular compartment, or formation of large aggregates that may affect protein function.

Here, we create a genetically encoded fluorescent biosensor to address these issues and enable the rapid detection of protein expression within live cells. We call our sensor STEP, for sensor for transiently expressed proteins (Figure 1a). Inspired by the GCaMP family of biosensors that enable fast detection of Ca^{2+} dynamics,[16] the STEP is based on a circularly permuted GFP (cpGFP) that can fold and mature independently of the protein of interest. In this cpGFP, the N- and C-termini are located in the middle of strand β7 of the β-barrel (Figure 1b), which creates a pore on the protein
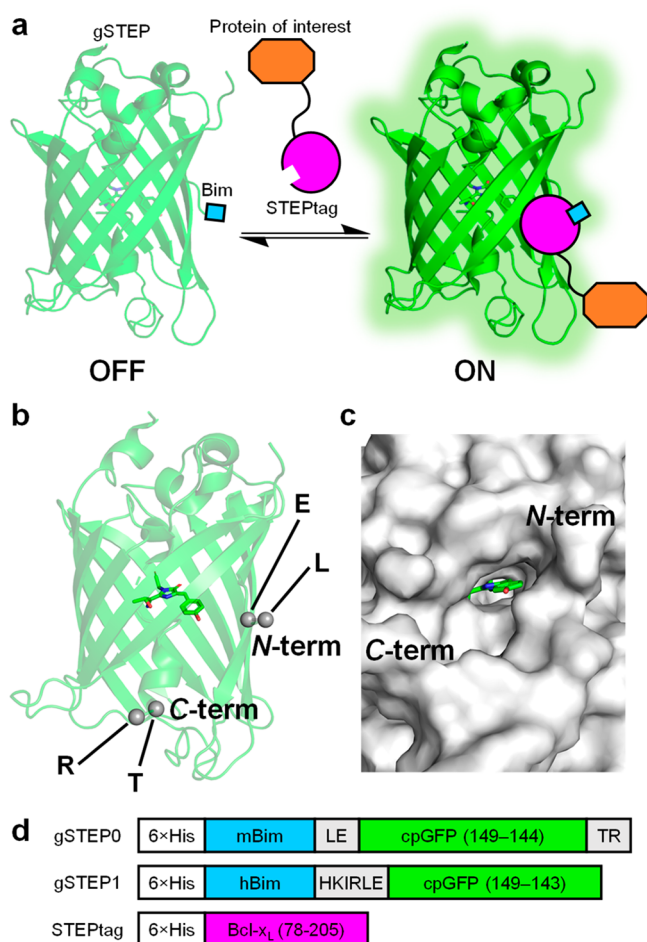
Figure 1. Sensor for transiently expressed proteins (STEP). (a) Cartoon representation of the STEP. A green fluorescent STEP (gSTEP) is expressed and allowed to mature before expression of a STEPtagged protein of interest (not to scale). Prior to STEPtag binding to the Bim peptide, gSTEP is dimly fluorescent (OFF), while the bound gSTEP emits a strong fluorescence signal (ON). (b) Crystal structure of the circularly permuted GFP from the GCaMP3 genetically encoded calcium indicator (PDB ID: 4IK8).[37] The chromophore is shown as sticks, and residues forming the N- and C-terminal amino acid linkers are shown as gray spheres and identified by their one-letter code. (c) Surface of the circularly permuted GFP shows a pore on the barrel surface next to the chromophore phenolate moiety (green sticks). (d) Schematic representation of gSTEP0, gSTEP1, and STEPtag. Linker sequences are shown in gray. Circularly permuted GFP (cpGFP) is shown in green, and residues are numbered according to the sequence of *Aequorea victoria* GFP. Bcl-x$_L$ is shown in magenta, and residues are numbered according to the UniProt sequence (Q07817). 6×His, mBim, and hBim indicate the histidine tag, mouse Bim, and human Bim peptides, respectively.

surface directly next to the chromophore phenolate moiety (Figure 1c). This pore exposes the chromophore to the solvent, resulting in quenched fluorescence (Figure 1a, OFF state).[17] A peptide, Bim, from the BH3 domain of the Bcl-2 family of eukaryotic apoptosis regulators[18] is genetically fused to the N-terminus of cpGFP, creating a green fluorescent STEP (gSTEP). This Bim peptide has no endogenous activity in *E. coli*,[19] but in our system it enables specific binding of a protein tag (STEPtag) derived from another Bcl-2 family protein, Bcl-x$_L$.[20] Formation of the gSTEP/STEPtag complex causes a change to the electrostatic environment of the chromophore, restoring bright fluorescence (Figure 1a, ON state). By expressing gSTEP and allowing its chromophore to mature before expression of the STEPtagged protein of interest is initiated, the biosensor is ready to detect its target as it is expressed and folded, helping to eliminate delays in detection of protein expression caused by maturation.

To create the first prototype of the sensor, gSTEP0, we fused the helical mouse Bim peptide (26 amino acids) to the cpGFP from the genetically encoded calcium indicator GCaMP3,[17] and retained the N- and C-terminal linkers on either side of the barrel pore (Leu-Glu and Thr-Arg, respectively), which have been shown to be important to the fluorescence response of these calcium sensors (Figure 1d, Supplementary Table S1).[16] The STEPtag (15.5 kDa) was created by truncating the N- and C-termini of human Bcl-x$_L$ (Figure 1d, Supplementary Table S1) to remove structural elements that are not essential for binding to Bim but can cause formation of a domain-swapped dimer,[21,22] and a hydrophobic membrane-anchor domain, respectively.[23,24] Addition of a saturating concentration of purified STEPtag to gSTEP0 resulted in an intensiometric fluorescence increase ($\Delta F/F_0$, calculated as $(F_{max} - F_{min})/F_{min}$) of 1.4 ± 0.1, with a dissociation constant (K_d) of 250 ± 40 nM (Supplementary Figure S1, Table 1). Interestingly, the Hill coefficient was found to be 2.9, implying that some form of cooperative binding is occurring, despite the expected 1:1 stoichiometry of the Bim-Bcl-x$_L$ pair. Nevertheless, control experiments where STEPtag was replaced with bovine serum albumin, or where gSTEP0 was replaced by cpGFP, confirmed that the fluorescence response of the biosensor was dependent on specific binding of the Bim peptide to the STEPtag (Supplementary Figure S1b,c).

Having established that gSTEP0 could be used to detect the presence of STEPtag *in vitro*, we next sought to improve the properties of our sensor. We began by truncating the C-terminus of gSTEP0 by removing the Thr-Arg linker (Figure 1d) as well as an additional 1 to 4 amino acids from cpGFP in order to increase the size of the pore on the barrel surface, which we hypothesized would improve $\Delta F/F_0$ by reducing background fluorescence through increased quenching in the

Table 1. Properties of STEP Variants

sensor	λ_{ex} (nm)^a	λ_{em} (nm)^a	$K_d{}^b$ (nM)	*in vitro* $\Delta F/F_0{}^b$	*in vivo* $\Delta F/F_0{}^c$	k_{on} (×10⁵M⁻¹ s⁻¹)^d	k_{off} (s⁻¹)^e
gSTEP0	496 ± 1	513 ± 1	250 ± 40	1.4 ± 0.1	N.D.^{f}	N.D.^{f}	N.D.^{f}
gSTEP1	504 ± 1	515 ± 1	120 ± 20	3.4 ± 0.4	11 ± 4	1.7 ± 0.2	0.020 ± 0.007

$^a n = 9$, mean ± s.d. For comparison, excitation and emission wavelengths of EGFP are 488 and 507 nm, respectively. ^{b}Measured in solution using purified gSTEP (75 nM) and STEPtag (up to 10 μM). For gSTEP0, $n = 6$, fit value ± 95% confidence interval. For gSTEP1, $n = 18$, fit value ± 95% confidence interval. ^{c}Calculated from the average fluorescence of individual cells expressing both gSTEP1 and STEPtag, or expressing only gSTEP1 (see Figure 3a). $n = 2$, mean ± s.d. ^{d}Measured in solution using purified gSTEP1 (1 μM) and STEPtag (5 μM), $n = 3$, fit value ± 95% confidence interval. ^{e}Calculated from the K_d and k_{on}. Error represents the propagated 95% confidence interval. ^{f}N.D. indicates not determined.

unbound state. The best truncated mutant, gSTEP0-T1, had both the Thr-Arg linker and a single additional amino acid from cpGFP removed (Supplementary Table S1), and we found that it bound specifically to STEPtag with a K_d of 210 ± 80 nM and a $\Delta F/F_0$ of 2.1 ± 0.4 (Supplementary Figure S2, Supplementary Table S2). Control experiments with this improved variant confirmed that fusion of STEPtag using a 10-amino acid linker to either the N- or C-terminus of a protein of interest does not substantially affect biosensor response or binding affinity (Supplementary Figure S3).

Next, we replaced the mouse Bim peptide of gSTEP0-T1 with the human homologue or a range of synthetic variants displaying tight binding to Bcl-x$_L$[25] which we hypothesized would enhance binding affinity to the STEPtag. Of these, the human Bim peptide performed the best (K_d = 170 ± 40 nM, $\Delta F/F_0$ = 3.3 ± 0.6, Supplementary Table S2). In parallel, we tested various linker lengths (1 to 5 amino acids) between the original mouse Bim peptide and cpGFP in gSTEP0-T1 to allow alternate binding poses of the STEPtag on the gSTEP surface upon formation of the complex. We hypothesized that changing the relative orientation of the binding partners could enhance binding affinity or $\Delta F/F_0$ by allowing more favorable noncovalent interactions between these molecules or causing a larger change to the electrostatic environment of the chromophore upon binding, respectively. We found that addition of a four-amino acid linker (gSTEP0-T1-L4) improved the binding affinity but not $\Delta F/F_0$ relative to gSTEP0-T1 (Supplementary Table S2). Interestingly, replacement of the mouse Bim peptide in gSTEP0-T1-L4 by its human homologue yielded a worse K_d and $\Delta F/F_0$ even though human Bim performed better than mouse Bim in gSTEP0-T1. Therefore, as a final step, we performed combinatorial saturation mutagenesis of the four-amino acid linker introduced between human Bim and cpGFP in gSTEP0-T1-L4, and screened the resulting library for improved brightness and $\Delta F/F_0$ using fluorescence-activated cell sorting and microplate-based binding assays, respectively (Methods). This yielded our final improved variant, gSTEP1 (Figure 1d, Table 1, Supplementary Table S1), which displays a $\Delta F/F_0$ of 3.4 ± 0.4, equivalent to that of the original GCaMP ($\Delta F/F_0$ = 3.5),[16] and is as bright as the enhanced GFP (EGFP) from *Aequorea victoria*[26] when fully bound to STEPtag (Figure 2a). gSTEP1 binds specifically (Figure 2b) and rapidly (Figure 2c) to STEPtag, with a K_d of 120 ± 20 nM and a binding rate constant (k_{on} = 1.7 ± 0.2 × 10^5 M^{-1} s^{-1}) that is comparable to that of peptide antigen binding by antibodies.[27]

Next, we evaluated whether gSTEP1 could be used to detect STEPtag expression in live *E. coli* cells, which we selected as a case study given the fast GFP maturation rate in this organism.[5] To do so, we prepared an *E. coli* strain that constitutively expresses a low basal concentration of gSTEP1 and in which STEPtag expression can be induced by the addition of arabinose (Methods). In flow cytometry experiments, we observed that cells constitutively expressing gSTEP1 and overexpressing STEPtag were considerably brighter than those that do not express the binding partner (Figure 3a), with little overlap between the fluorescence distributions of the two cell populations. Under these conditions, the mean fluorescence of the cellular population in the ON state was an order of magnitude higher than that of the cellular population in the OFF state, resulting in a $\Delta F/F_0$ of 11 ± 4 (Table 1). Taken together, these results demonstrate that the fluorescence difference of gSTEP1 in the ON and OFF states is sufficient to
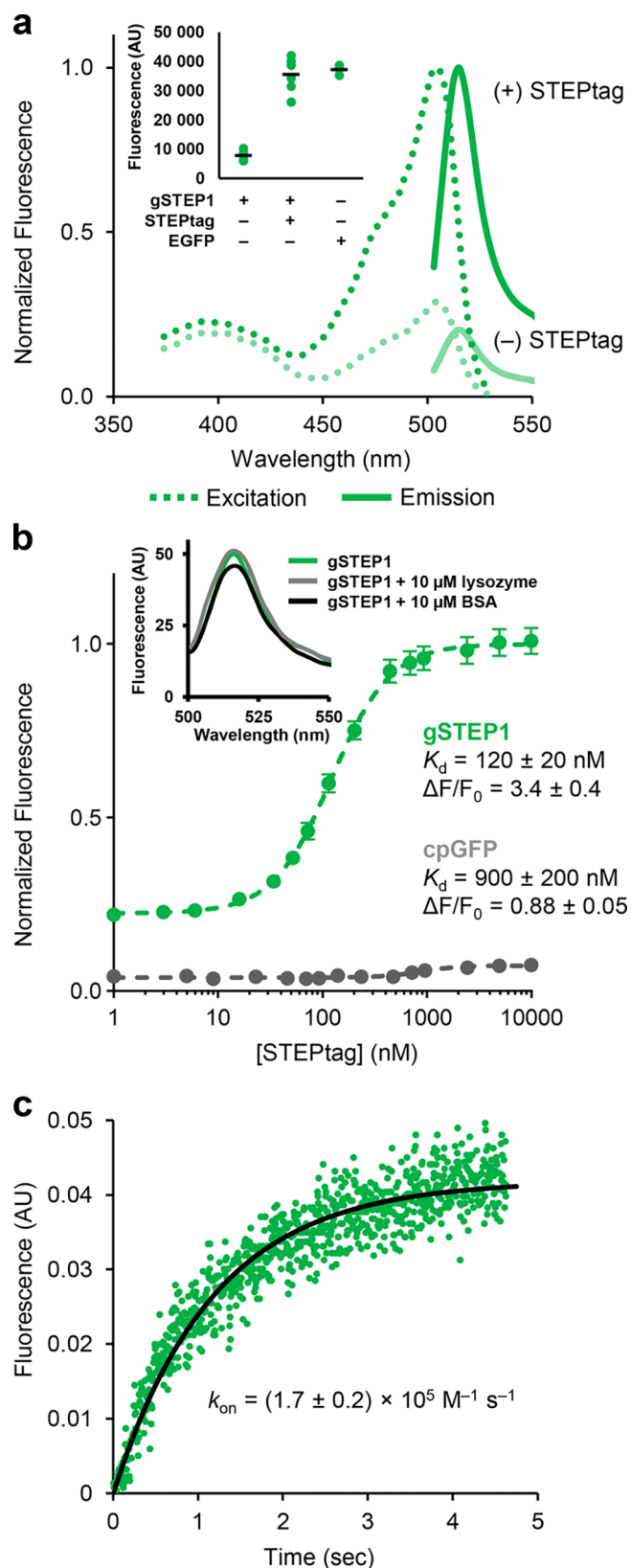

Figure 2. *In vitro* characterization of gSTEP1. All assays were performed in 20 mM sodium phosphate buffer containing 50 mM NaCl (pH 7.4). (a) Normalized excitation (λ_{em} = 550 nm, dotted line) and emission (λ_{ex} = 485 nm, full line) spectra of gSTEP1 (75 nM) in the presence or absence of saturating STEPtag (10 μM). n = 3, average spectra shown. Inset: the fluorescence intensity at 515 nm (λ_{ex} = 485 nm) of gSTEP1, in the presence or absence of saturating

Figure 2. continued

STEPtag, compared to 75 nM EGFP. $n = 6$ for gSTEP1, $n = 3$ for EGFP, mean values are shown as black lines. (b) Binding curves of 75 nM gSTEP1 (green) or cpGFP (gray) with STEPtag. Fluorescence is normalized to the maximum intensity observed for gSTEP1. Dashed lines represent fits of the Hill equation to the data (Hill coefficients of 1.5 or 2.2 for gSTEP1 or cpGFP, respectively). For the gSTEP1 binding curve, $n = 18$, mean ± SEM shown. For cpGFP, $n = 3$, mean value shown. K_d and $\Delta F/F_0$ values were obtained from the fit and indicated with the 95% confidence interval around the fit values. Inset: emission spectra ($\lambda_{ex} = 485$ nm) of 75 nM gSTEP1 alone and in the presence of 10 μM hen egg white lysozyme or bovine serum albumin (BSA). $n = 3$, average spectra shown. (c) Rapid-mixing stopped-flow binding kinetics of a representative replicate of gSTEP1 mixed with saturating STEPtag. The black line represents a fit of the integrated rate equation to the data (Methods).

distinguish individual bacterial cells that express STEPtag from those that do not.

Having demonstrated that gSTEP1 could be used to detect the STEPtag in live *E. coli* cells at the steady-state, we evaluated the ability of the biosensor to report on STEPtag concentration dynamics. To do so, we cultured the cells constitutively expressing gSTEP1 until they reached the exponential growth phase, and then induced expression of STEPtag by adding arabinose. We observed an immediate fluorescence increase (Figure 3b), and the signal continued to increase linearly for 20 min. Control experiments demonstrated that it was possible to modulate the rate of fluorescence increase by reducing the amount of arabinose added, thereby lowering the rate of STEPtag production (Supplementary Figure S4). We also demonstrated that any metabolic load from the presence of constitutively expressed gSTEP1 had a minimal effect on arabinose-induced protein expression (Supplementary Figure S5). To determine how long it takes for protein expression to be detected by our biosensor, we measured the baseline fluorescence of these cells prior to induction of STEPtag expression, and used the noise in this baseline data to set detection thresholds above the signal at time of induction ($t = 0$ min). The standard deviation was used to quantify the noise, such that the thresholds of 1, 2, and 3 standard deviations above the signal at $t = 0$ min represent increasing levels of confidence that the increase in fluorescence is due to the fluorescent reporter (Table 2). For cells expressing both gSTEP1 and STEPtag, the threshold of 3 standard deviations of the baseline above the signal at 0 min was reached in 1.6 ± 0.2 min. By contrast, when we induced expression of EGFP (maturation half-time = 25 min[26]) using the same promoter in cells containing only the EGFP expression vector, it took 4 ± 1 min for it to reach the same threshold, over twice as long as for gSTEP1. Of note, the rate of fluorescence increase for EGFP accelerated with time, reaching a steady state after approximately 10 min under these conditions. Presence of this lag phase is consistent with slower oxidation than folding/cyclization/dehydration during GFP chromophore maturation.[28] In the first 5 min following induction of protein expression, gSTEP1 provided 6- to 10-fold higher fluorescence signal than EGFP, and this signal remained higher for over 20 min (Figure 3). We also tested Superfolder GFP (sfGFP), which folds and matures faster than EGFP (maturation half-time = 13.6 min[29]). Expression of sfGFP using the same promoter also resulted in a lag phase, albeit shorter than the one observed for EGFP (approximately
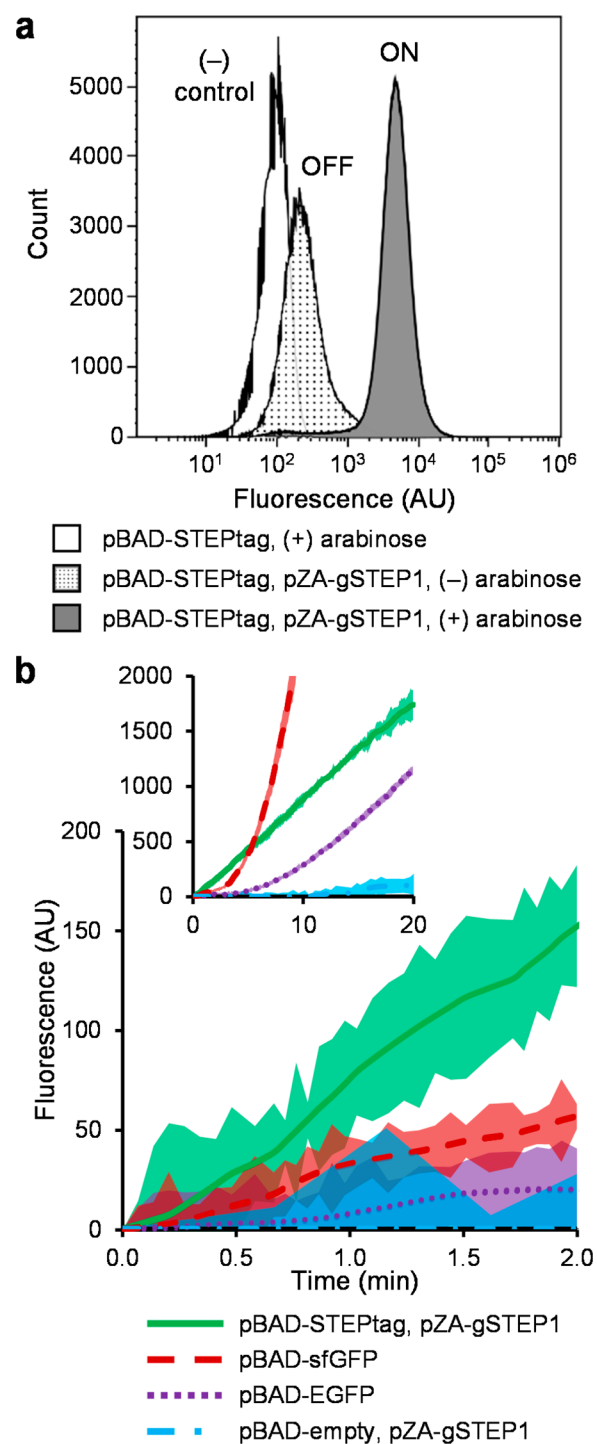

Figure 3. gSTEP1 enables rapid detection of protein expression in live bacterial cells. (a) Flow cytometry histograms of a representative biological replicate of gSTEP1 fluorescence in live *E. coli* cells expressing only STEPtag (negative control), gSTEP1 (OFF state), or both (ON state). The pZA vector constitutively expresses gSTEP1, while STEPtag expression from the pBAD vector is induced using 0.2% arabinose. (b) Time course of protein expression in live *E. coli*. Cells were grown to the end of the exponential growth phase (OD$_{600}$ = 1.1), then fluorescence was measured immediately after pBAD vectors containing either STEPtag (for cells constitutively expressing gSTEP1), EGFP, or sfGFP were induced with 0.45% arabinose. Each data set was blanked by the fluorescence signal at 0 min, and smoothed by three passes through a seven-point moving average filter. $n = 4$, the shaded area represents the mean ± s.d. A negative control experiment is also shown, where cells constitutively expressing

Figure 3. continued

gSTEP1 have an empty pBAD vector induced (pBAD-empty, pZA-gSTEP1). These cells were grown to OD_{600} of 0.6, and the shaded area represents the mean ± s.d. for $n = 3$. Inset: the same time course is shown, extended to 20 min to show the effects of longer-term induction. The same color scheme is used as in the main figure.

Table 2. Time Required to Reach a Specified Level of Fluorescence Following Induction of Protein Expression in Live *E. coli* Cells

fluorescent reporter[a]	time to reach X standard deviations above initial fluorescence intensity (min)[b]		
	$X = 1$	$X = 2$	$X = 3$
gSTEP1	0.63 ± 0.03	1.09 ± 0.06	1.6 ± 0.2
EGFP	1.21 ± 0.09	3 ± 2	4 ± 1
sfGFP	1.1 ± 0.4	2.1 ± 0.6	2.9 ± 0.4

[a]gSTEP1 refers to cells expressing both gSTEP1 and STEPtag. EGFP and sfGFP refer to cells expressing only EGFP or sfGFP. STEPtag, EGFP, and sfGFP expression is under control of the araBAD promoter, and can be induced using arabinose. gSTEP1 is constitutively expressed. [b]Fluorescence of the bacterial cell population was measured for 10 min before induction of STEPtag, EGFP, or sfGFP expression using 0.45% arabinose, and this baseline signal was used to calculate the standard deviation serving as detection threshold ($n = 4$, mean ± s.d.).

5 min to reach steady-state), and yielded a fluorescence intensity increase of 3 standard deviations above the initial signal in 2.9 ± 0.4 min (Table 2). These results demonstrate that gSTEP1 enables faster detection of protein expression in live *E. coli* cells than the use of traditional GFP reporters, which should increase the temporal resolution of experiments aiming to detect transiently expressed proteins or other fast biological processes.

Compared with other genetically encoded fluorescent biosensors used to track protein expression in real-time, gSTEP1 has the benefits of not requiring the use of protein translocation[11,12] or formation of large protein aggregates,[14] which should cause minimal perturbation to the subcellular localization and physical properties of the protein of interest. In the course of this work, a protein biosensor operating on a similar principle to the STEP was published.[30] This sensor, called Flashbody, is based on a cpGFP that is inserted between heavy and light chain fragments from the variable region of an antibody, which together bind specifically to a 7-amino acid peptide tag fused to a protein of interest. Like gSTEP1, the Flashbody has the benefits of not requiring translocation or formation of large aggregates, and the response of the two biosensors to their respective binding partner is similar ($\Delta F/F_0 \approx 3$). However, gSTEP1 displays tighter binding (K_d of 120 nM for gSTEP1 *vs* 423 nM for the Flashbody), which could allow detection of proteins present at lower concentrations than the Flashbody limit of detection, and binds to its partner with a rate constant 2 orders of magnitude higher than that of the Flashbody (k_{on} of 1.7×10^5 M^{-1} s^{-1} for gSTEP1 *vs* 3.38×10^3 M^{-1} s^{-1} for Flashbody).[30] Taken together, these advantages of gSTEP1 make it a useful alternative to other biosensors for the rapid detection of protein expression *in vivo* and in real time.

In conclusion, we have developed a genetically encoded fluorescent biosensor to rapidly detect protein expression within live bacterial cells. Because it is based on a circularly permuted GFP, our sensor should be compatible with a wide range of experimental setups. However, for some applications, it may be necessary to further improve the biosensor's dynamic range and sensitivity. This could be achieved by replacing the Bim/STEPtag pair by alternate binding partners, and optimizing the fluorescence response by random mutagenesis followed by rounds of fluorescence-activated cell sorting using the pZA-gSTEP1/pBAD-STEPtag strain developed here to allow modulation of the STEPtag concentration. Alternate colors should also be possible *via* the use of circularly permuted yellow[31] or red[32] fluorescent proteins. We expect that the engineering of a color palette of orthogonal STEP biosensors will enable multiplexing for more complex imaging experiments, opening the door to the *in vivo* visualization of protein concentration dynamics in real time and at unprecedented spatiotemporal resolution.

■ METHODS

Chemicals and Enzymes. All reagents used were of the highest available purity. Synthetic oligonucleotides were purchased from Eurofins MWG Operon. Restriction enzymes and DNA-modifying enzymes were purchased from New England Biolabs. All aqueous solutions were prepared using water purified with a Barnstead Nanopure Diamond system.

Mutagenesis and Cloning. Codon-optimized (*E. coli*) and his-tagged (N-terminus) sequences for gSTEP0 and STEPtag (Supplementary Table S1) were purchased from ATUM. Truncation mutants of gSTEP0 (T1−T4) were obtained by polymerase chain reaction amplification of the appropriate region of the gene, while mutants with added linkers (L1−L5) or alternate Bim peptides (hBim, XXA1, XXA4, G2gE, Y4eK) were generated using splicing by overlap extension (SOE) mutagenesis (Supplementary Table S3).[33] Briefly, for each mutagenesis step, two oligonucleotides containing the desired mutations were ordered, one complementary to each strand of the template gene. Each of these mutagenesis oligonucleotides was used in conjunction with a flanking oligonucleotide, complementary to either the 5′ or 3′ end of the template gene. Polymerase chain reaction amplification of the template sequence using these two pairs of oligonucleotides generated two DNA fragments that overlap at the mutagenesis site. An equimolar mixture of these two fragments was then further amplified using the two flanking oligonucleotides, resulting in a complete gene sequence having incorporated the mutations present in the mutagenesis oligonucleotides. Amplification was performed using Vent DNA Polymerase (New England Biolabs), following the manufacturer's protocol. The combinatorial linker saturation library was generated by SOE mutagenesis of gSTEP0-T1-L4 using oligonucleotides containing four consecutive NNS degenerate codons, one for every position of the linker sequence. All sequences were subcloned into pET11a vectors (Novagen) *via* the *Nde*I/*Bam*HI restriction sites. Gene constructs for live-cell experiments (*i.e.*, flow cytometry and *in vivo* binding assays) were subcloned *via* *Nco*I/*Eco*RI or *Hind*III/*Bam*HI into either the pBAD/His A (Invitrogen) or pZA23MCS (EXPRESSYS) vectors for inducible or constitutive expression, respectively.

Aequorea victoria EGFP [Genbank AAB02572] was cloned into pBAD/His A using *Xho*I/*Eco*RI, which added the pBAD His tag/Xpress Epitope/EK site to the N-terminus. His-tagged (C-terminus) *Thermoascus aurantiacus* xylanase 10A (TAX, UniProtKB: P23360) in which the two catalytic residues were

mutated to alanine (E157A/E263A) cloned into a pET11a vector *via* NdeI/BamHI was a gift from Stephen L. Mayo.[34] TAX-L10-STEPtag and STEPtag-L10-TAX constructs were generated using SOE mutagenesis and cloned into pET11a vectors as described above. His-tagged (N-terminus) sfGFP cloned into a pBAD vector (pBAD-sfGFP)[29] was a gift from Michael Davidson and Geoffrey Waldo (Addgene plasmid #54519; http://n2t.net/addgene:54519; RRID: Addgene_54519). All constructs were verified by sequencing the entire open reading frame (see Supplementary Table S1 for amino acid sequences), and transformed into either BL21-Gold(DE3) (Agilent) or TOP10 (Thermo Fisher) chemically competent *E. coli* cells for pET11a, or pBAD and pZA vectors, respectively.

Protein Expression and Purification. Transformed *E. coli* cells harboring expression vectors were grown in 500 mL lysogeny broth (LB) supplemented with 100 μg mL^{-1} ampicillin at 37 °C with shaking. When an OD$_{600}$ of 0.6−0.8 was reached, protein expression was induced by addition of 1 mM isopropyl β-D-1-thiogalactopyranoside (pET11a vectors) or 0.2% arabinose (pBAD vectors). Following overnight incubation at 16 °C with shaking, cells were harvested by centrifugation and lysed with an EmulsiFlex-B15 cell disruptor (Avestin). Following removal of cellular debris by centrifugation, proteins were extracted and purified by immobilized metal affinity chromatography using Profinity IMAC resin (Bio-Rad) in a gravity flow column according to the manufacturer's protocol. Eluted proteins were exchanged into 20 mM sodium phosphate buffer containing 50 mM NaCl (pH 7.4) and concentrated using Amicon Ultra-15 centrifugal filters with a molecular weight cutoff of 3 kDa (Millipore) for STEPtag, or Microsep Advance centrifugal filters with a molecular weight cutoff of 10 kDa (Pall) for all other proteins. Purified proteins were quantified by measuring absorbance at 280 nm in a 1 cm quartz cuvette with a SpectraMax Plus384 microplate spectrophotometer (Molecular Devices), and applying Beer−Lambert's law using extinction coefficients calculated with the ProtParam tool (https://web.expasy.org/protparam/).

***In Vitro* Binding Assays.** All fluorescence measurements were performed in Fluotrac 96-well plates (Greiner Bio-One) on a Tecan Infinite M1000 plate reader using 75 nM of each gSTEP variant in 20 mM sodium phosphate buffer containing 50 mM NaCl (pH 7.4). To calculate K_d and $\Delta F/F_0$ values, gSTEP fluorescence intensity (λ_{ex} = 485 nm, λ_{em} = 515 nm) as a function of STEPtag, TAX-L10-STEPtag, STEPtag-L10-TAX, or control protein concentration (*e.g.*, bovine serum albumin [Bio-Rad] or an inactive mutant of *Thermoascus aurantiacus* xylanase 10A purified as described above[34]) was fit to the Hill equation, accounting for ligand depletion:[35]

$$\frac{[AB_{eq}]}{[A_0]} = \frac{(K_d + [A_0] + [B_0]) - \sqrt{(K_d + [A_0] + [B_0])^2 - 4[A_0][B_0]}}{2[A_0]}$$

where *A* (gSTEP variants) and *B* (STEPtag, TAX-L10-STEPtag, or STEPtag-L10-TAX) are the two binding proteins, and $[A_0]$ and $[B_0]$ are the initial concentrations of each protein. $[AB_{eq}]$ is the equilibrium concentration of the bound complex. For each experiment, a minimum of three replicates were performed.

Fluorescence-Activated Cell Sorting. To improve the signal-to-noise ratio in live cells, we aimed to isolate gSTEP0-T1-L4 variants that gave the brightest fluorescence from the linker saturation library. To do so, we transformed the gSTEP0-T1-L4 mutant library into *E. cloni* Elite electrocompetent *E. coli* cells (Lucigen), which were plated on LB agar supplemented with 100 μg mL^{-1} ampicillin. Following overnight incubation at 37 °C, a total of 10^5 colonies from multiple agar plates were collected, pooled together, and cultured overnight in 10 mL LB supplemented with ampicillin. Following extraction of plasmid DNA from this culture, the library was transformed into BL21-Gold(DE3) electrocompetent *E. coli* cells, and plated on LB agar supplemented with ampicillin. From these plates, 10^5 colonies were collected, pooled together, and cultured overnight in 10 mL LB supplemented with ampicillin. This bacterial culture was diluted 100-fold into fresh LB supplemented with ampicillin and grown to an OD$_{600}$ of 0.5−0.9. Because the leaky expression of the T7 RNA polymerase in BL21-Gold(DE3) provided sufficient quantities of protein to screen, the cells were not further induced with isopropyl β-D-1-thiogalactopyranoside to limit their metabolic burden. After growth, cells were centrifuged and pellets were washed twice with filter-sterilized 20 mM sodium phosphate buffer containing 50 mM NaCl (pH 7.4). Resuspended cells were diluted in this buffer to a concentration of approximately 5 × 10^7 colony forming units per mL.[36] The cells were then filtered twice using a 40-μm Falcon Cell Strainer (Fisher) to remove large particulates. Fluorescence-activated cell sorting was performed on a MoFlo AstriosEQ Cell Sorter (Beckman Coulter) using a 488 nm laser for excitation and a 513/26 nm filter for detecting fluorescence emission. Data analysis was performed with the FlowJo software package (BD). This process was repeated twice in succession, collecting 20 000 of the brightest cells each time.

The collected cells were used to inoculate 50 mL of fresh LB supplemented with ampicillin, and grown overnight at 37 °C with shaking. This culture was used to streak an LB agar plate supplemented with ampicillin. From this plate, 96 colonies were picked into individual wells of a Nunc V96 MicroWell polypropylene plate containing 200 μL of LB with 100 μg mL^{-1} ampicillin supplemented with 10% glycerol. The plate was covered with a sterile gas permeable rayon film (VWR) and incubated overnight at 37 °C with shaking. After incubation, the mother plate was used to inoculate duplicate Nunc V96 MicroWell polypropylene plates (daughter plates) containing 250 μL of LB with 100 μg mL^{-1} ampicillin per well. Daughter plates were sealed with rayon film and incubated overnight (37 °C, 250 rpm shaking). After incubation, the cells were harvested by centrifugation and the pellets were washed twice with phosphate buffered saline. These pellets were resuspended and lysed in 100 μL of Bugbuster protein extraction reagent (Millipore) containing 5 U mL^{-1} Benzonase nuclease (Millipore) and 1 mg mL^{-1} hen egg white lysozyme (Omnipure). Following centrifugation to remove cellular debris, the clarified lysate (30 μL) was transferred to a Fluotrac 96-well plate (Greiner Bio-One) for screening. To each 30-μL lysate containing a different gSTEP0-T1-L4

variant, 150 μL of 20 mM sodium phosphate buffer containing 50 mM NaCl (pH 7.4) and 0 or 9 μM purified STEPtag was added. Fluorescence was measured with a Tecan Infinite M1000 plate reader. Emission spectra (λ_{ex} = 485 nm) were measured from 500 to 560 nm. From these spectra, $\Delta F/F_0$ was calculated for each protein variant, and the one with the best response (gSTEP1) was analyzed further.

Rapid-Mixing Stopped-Flow Kinetics. Measurements were performed using an RSM 1000 UV−vis rapid-scanning spectrophotometer (Olis) equipped with a 1.24 mm-slit fixed disk for single wavelength measurements, and plane gratings with 400 lines mm^{-1} and a 500 nm blaze wavelength. All other fixed slits were set to 3.16 mm to maximize signal. Purified gSTEP1 (1 μM) and STEPtag (5 μM) were loaded into the spectrophotometer, which was kept at 37 °C using a temperature control unit (Julabo). 300 μL of each sample was pumped into the mixing chamber, and the fluorescence was measured (λ_{ex} = 485 nm, λ_{em} = 515 nm). For each combination of samples, the dead volume was cleared prior to data collection. Control experiments were performed to confirm that fluorescence increase was due to binding of gSTEP1 to STEPtag (Supplementary Figure S6). The data was fit to the integrated rate equation, accounting for ligand depletion,[35]

$$[AB] = \frac{x \cdot y (e^{(x-y)k_{on}t} - 1)}{(xe^{(x-y)k_{on}t} - y)}$$

where A and B are the two binding proteins (gSTEP1 and STEPtag), $x = [AB_{eq}]$, $y = [A_0][B_0]/[AB_{eq}]$, and t is the time. Three replicates were measured for this experiment, and the data from all replicates were used for the fit.

Flow Cytometry. TOP10 *E. coli* cells (Invitrogen) transformed with pZA-gSTEP1 and/or pBAD-STEPtag vectors were cultured in 50 mL LB supplemented with 100 μg mL^{-1} ampicillin (for cells containing pBAD) and/or 50 μg mL^{-1} kanamycin (for cells containing pZA). Cells were grown with shaking at 37 °C to an OD$_{600}$ of 0.4−0.8, then the culture containing both pBAD-STEPtag and pZA-gSTEP1 was split equally into two flasks, one to be induced and the other to be left uninduced. Following induction of cells containing pBAD vectors with 0.2% arabinose, cultures were incubated for an additional 60 min at 37 °C with shaking. Cells were then harvested by centrifugation, and prepared for flow cytometry as described in the cell sorting protocol above. Two biological replicates of flow cytometry measurements were performed using a Gallios flow cytometer (Beckman Coulter), set to detect either 50 000 or 500 000 events per run. Fluorescence was detected with a 525/40 filter (λ_{ex} = 488 nm), and data analysis was performed using the Kaluza software package (Beckman Coulter).

***In Vivo* Binding Assays.** TOP10 *E. coli* cells transformed with the appropriate vectors were cultured as described for the flow cytometry experiments above. Cells were grown with shaking at 37 °C to an OD$_{600}$ of 0.6−1.1, after which 200 μL of each culture was transferred to a Fluotrac 96-well plate (Greiner Bio-One). Fluorescence measurements were recorded on an Infinite M1000 microplate reader equipped with an injector module (Tecan), preheated to 37 °C (λ_{ex} = 488 nm, λ_{em} = 514 nm). Measurements were taken every 2 min for 10 min, shaking the plate before each measurement, then protein expression was induced by injecting 12 μL of 8% arabinose into the wells (final concentration of 0.45%), followed by 3 s of

shaking and 2 s of settle time. Fluorescence was measured every 2−6 s for an additional 20 or 40 min. For each experiment, a minimum of three replicates were performed.

■ ASSOCIATED CONTENT

Ⓢ Supporting Information

The Supporting Information is available free of charge at https://pubs.acs.org/doi/10.1021/acssynbio.0c00407.

> Amino acid sequences, *in vitro* results for all constructs tested, mutagenesis primer sequences, *in vitro* characterization of gSTEP0 and gSTEP-T1 with BSA controls for specific binding, binding curves for STEPtag-TAX fusions, time courses in live *E. coli* with varying arabinose concentrations and plasmid controls (PDF)

■ AUTHOR INFORMATION

Corresponding Author

Roberto A. Chica − *Department of Chemistry and Biomolecular Sciences, University of Ottawa, Ottawa, Ontario K1N 6N5, Canada;* ⦿ orcid.org/0000-0003-3789-9841; Email: rchica@uottawa.ca

Authors

Matthew G. Eason − *Department of Chemistry and Biomolecular Sciences, University of Ottawa, Ottawa, Ontario K1N 6N5, Canada*

Antonia T. Pandelieva − *Department of Chemistry and Biomolecular Sciences, University of Ottawa, Ottawa, Ontario K1N 6N5, Canada*

Marc M. Mayer − *Department of Chemistry and Biomolecular Sciences, University of Ottawa, Ottawa, Ontario K1N 6N5, Canada*

Safwat T. Khan − *Department of Chemistry and Biomolecular Sciences, University of Ottawa, Ottawa, Ontario K1N 6N5, Canada*

Hernan G. Garcia − *Biophysics Graduate Group, Department of Physics, Department of Molecular and Cell Biology, and Institute for Quantitative Biosciences-QB3, University of California, Berkeley, Berkeley, California 94720, United States*

Complete contact information is available at:
https://pubs.acs.org/10.1021/acssynbio.0c00407

Author Contributions

R.A.C. and H.G.G. conceived the project. M.G.E and S.T.K. created the gene sequences. M.G.E. and A.T.P. engineered proteins and characterized their properties. M.G.E. and M.M.M. performed flow cytometry and *in vivo* binding assays. All authors analyzed data. M.G.E. and R.A.C. wrote the manuscript. H.G.G. edited the manuscript.

Notes

The authors declare no competing financial interest.
Plasmids containing STEPtag, STEPtag-L10-TAX, TAX-L10-STEPtag, and gSTEP1 are available from Addgene (Plasmids #159373−159376).

■ ACKNOWLEDGMENTS

■ ABBREVIATIONS

GFP, green fluorescent protein; STEP, sensor for transiently expressed proteins; cpGFP, circularly permuted green fluorescent protein; gSTEP, green fluorescent sensor for transiently expressed proteins; EGFP, enhanced green fluorescent protein; sfGFP, superfolder green fluorescent protein; SOE, splicing by overlap extension; LB, lysogeny broth.

■ REFERENCES

(1) Guet, C. C., Elowitz, M. B., Hsing, W., and Leibler, S. (2002) Combinatorial synthesis of genetic networks. *Science 296*, 1466−1470.

(2) Nielsen, A. A. K., Der, B. S., Shin, J., Vaidyanathan, P., Paralanov, V., Strychalski, E. A., Ross, D., Densmore, D., and Voigt, C. A. (2016) Genetic circuit design automation. *Science 352*, aac7341.

(3) Matsumoto, Y., Ito, Y., Tsuru, S., Ying, B.-W., and Yomo, T. (2011) Bacterial cells carrying synthetic dual-function operon survived starvation. *J. Biomed. Biotechnol. 2011*, 489265.

(4) Tsien, R. Y. (1998) The green fluorescent protein. *Annu. Rev. Biochem. 67*, 509−544.

(5) Balleza, E., Kim, J. M., and Cluzel, P. (2018) Systematic characterization of maturation time of fluorescent proteins in living cells. *Nat. Methods 15*, 47−51.

(6) Griffith, K. L., Shah, I. M., and Wolf, R. E., Jr (2004) Proteolytic degradation of Escherichia coli transcription activators SoxS and MarA as the mechanism for reversing the induction of the superoxide (SoxRS) and multiple antibiotic resistance (Mar) regulons. *Mol. Microbiol. 51*, 1801−1816.

(7) Tilly, K., Spence, J., and Georgopoulos, C. (1989) Modulation of stability of the Escherichia coli heat shock regulatory factor sigma. *J. Bacteriol. 171*, 1585−1589.

(8) Gedeon, T., and Bokes, P. (2012) Delayed protein synthesis reduces the correlation between mRNA and protein fluctuations. *Biophys. J. 103*, 377−385.

(9) Wang, X., Errede, B., and Elston, T. C. (2008) Mathematical analysis and quantification of fluorescent proteins as transcriptional reporters. *Biophys. J. 94*, 2017−2026.

(10) Berezhkovskii, A. M., and Shvartsman, S. Y. (2014) On the GFP-based analysis of dynamic concentration profiles. *Biophys. J. 106*, L13−15.

(11) Aymoz, D., Wosika, V., Durandau, E., and Pelet, S. (2016) Real-time quantification of protein expression at the single-cell level via dynamic protein synthesis translocation reporters. *Nat. Commun. 7*, 11304.

(12) Bothma, J. P., Norstad, M. R., Alamos, S., and Garcia, H. G. (2018) LlamaTags: A Versatile Tool to Image Transcription Factor Dynamics in Live Embryos. *Cell 173*, 1810−1822.

(13) Zhao, N., Kamijo, K., Fox, P. D., Oda, H., Morisaki, T., Sato, Y., Kimura, H., and Stasevich, T. J. (2019) A genetically encoded probe for imaging nascent and mature HA-tagged proteins in vivo. *Nat. Commun. 10*, 2947.

(14) Tanenbaum, M. E., Gilbert, L. A., Qi, L. S., Weissman, J. S., and Vale, R. D. (2014) A protein-tagging system for signal amplification in gene expression and fluorescence imaging. *Cell 159*, 635−646.

(15) Boersma, S., Khuperkar, D., Verhagen, B. M. P., Sonneveld, S., Grimm, J. B., Lavis, L. D., and Tanenbaum, M. E. (2019) Multi-Color Single-Molecule Imaging Uncovers Extensive Heterogeneity in mRNA Decoding. *Cell 178*, 458−472.

(16) Nakai, J., Ohkura, M., and Imoto, K. (2001) A high signal-to-noise Ca(2+) probe composed of a single green fluorescent protein. *Nat. Biotechnol. 19*, 137−141.

(17) Tian, L., Hires, S. A., Mao, T., Huber, D., Chiappe, M. E., Chalasani, S. H., Petreanu, L., Akerboom, J., McKinney, S. A., Schreiter, E. R., Bargmann, C. I., Jayaraman, V., Svoboda, K., and Looger, L. L. (2009) Imaging neural activity in worms, flies and mice with improved GCaMP calcium indicators. *Nat. Methods 6*, 875−881.

(18) O'Connor, L., Strasser, A., O'Reilly, L. A., Hausmann, G., Adams, J. M., Cory, S., and Huang, D. C. (1998) Bim: a novel member of the Bcl-2 family that promotes apoptosis. *EMBO J. 17*, 384−395.

(19) Pang, X., Moussa, S. H., Targy, N. M., Bose, J. L., George, N. M., Gries, C., Lopez, H., Zhang, L., Bayles, K. W., Young, R., and Luo, X. (2011) Active Bax and Bak are functional holins. *Genes Dev. 25*, 2278−2290.

(20) Muchmore, S. W., Sattler, M., Liang, H., Meadows, R. P., Harlan, J. E., Yoon, H. S., Nettesheim, D., Chang, B. S., Thompson, C. B., Wong, S. L., Ng, S. L., and Fesik, S. W. (1996) X-ray and NMR structure of human Bcl-xL, an inhibitor of programmed cell death. *Nature 381*, 335−341.

(21) Oberstein, A., Jeffrey, P. D., and Shi, Y. (2007) Crystal structure of the Bcl-XL-Beclin 1 peptide complex: Beclin 1 is a novel BH3-only protein. *J. Biol. Chem. 282*, 13123−13132.

(22) Kvansakul, M., Yang, H., Fairlie, W. D., Czabotar, P. E., Fischer, S. F., Perugini, M. A., Huang, D. C., and Colman, P. M. (2008) Vaccinia virus anti-apoptotic F1L is a novel Bcl-2-like domain-swapped dimer that binds a highly selective subset of BH3-containing death ligands. *Cell Death Differ. 15*, 1564−1571.

(23) Chen-Levy, Z., and Cleary, M. L. (1990) Membrane topology of the Bcl-2 proto-oncogenic protein demonstrated in vitro. *J. Biol. Chem. 265*, 4929−4933.

(24) Nguyen, M., Millar, D. G., Yong, V. W., Korsmeyer, S. J., and Shore, G. C. (1993) Targeting of Bcl-2 to the mitochondrial outer membrane by a COOH-terminal signal anchor sequence. *J. Biol. Chem. 268*, 25265−25268.

(25) Dutta, S., Ryan, J., Chen, T. S., Kougentakis, C., Letai, A., and Keating, A. E. (2015) Potent and specific peptide inhibitors of human pro-survival protein Bcl-xL. *J. Mol. Biol. 427*, 1241−1253.

(26) Cormack, B. P., Valdivia, R. H., and Falkow, S. (1996) FACS-optimized mutants of the green fluorescent protein (GFP). *Gene 173*, 33−38.

(27) Landry, J. P., Ke, Y., Yu, G. L., and Zhu, X. D. (2015) Measuring affinity constants of 1450 monoclonal antibodies to peptide targets with a microarray-based label-free assay platform. *J. Immunol. Methods 417*, 86−96.

(28) Reid, B. G., and Flynn, G. C. (1997) Chromophore Formation in Green Fluorescent Protein. *Biochemistry 36*, 6786−6791.

(29) Pedelacq, J. D., Cabantous, S., Tran, T., Terwilliger, T. C., and Waldo, G. S. (2006) Engineering and characterization of a superfolder green fluorescent protein. *Nat. Biotechnol. 24*, 79−88.

(30) Wongso, D., Dong, J., Ueda, H., and Kitaguchi, T. (2017) Flashbody: A Next Generation Fluobody with Fluorescence Intensity Enhanced by Antigen Binding. *Anal. Chem. 89*, 6719−6725.

(31) Baird, G. S., Zacharias, D. A., and Tsien, R. Y. (1999) Circular permutation and receptor insertion within green fluorescent proteins. *Proc. Natl. Acad. Sci. U. S. A. 96*, 11241−11246.

(32) Carlson, H. J., Cotton, D. W., and Campbell, R. E. (2010) Circularly permuted monomeric red fluorescent proteins with new termini in the beta-sheet. *Protein Sci. 19*, 1490−1499.

(33) Horton, R. M., Ho, S. N., Pullen, J. K., Hunt, H. D., Cai, Z., and Pease, L. R. (1993) Gene splicing by overlap extension. *Methods Enzymol.* 217, 270−279.

(34) Privett, H. K., Kiss, G., Lee, T. M., Blomberg, R., Chica, R. A., Thomas, L. M., Hilvert, D., Houk, K. N., and Mayo, S. L. (2012) Iterative approach to computational enzyme design. *Proc. Natl. Acad. Sci. U. S. A.* 109, 3790−3795.

(35) Hulme, E. C., and Trevethick, M. A. (2010) Ligand binding assays at equilibrium: validation and interpretation. *Br. J. Pharmacol.* 161, 1219−1237.

(36) Myers, J. A., Curtis, B. S., and Curtis, W. R. (2013) Improving accuracy of cell and chromophore concentration measurements using optical density. *BMC Biophys.* 6, 4.

(37) Chen, Y., Song, X., Ye, S., Miao, L., Zhu, Y., Zhang, R. G., and Ji, G. (2013) Structural insight into enhanced calcium indicator GCaMP3 and GCaMPJ to promote further improvement. *Protein Cell* 4, 299−309.